Controlling Of The Electric Field Profile In The Miniband Semiconductors In The Presence Of THz Bloch Oscillations

V.A. Maksimenko[1], V.V. Makarov[1], A.A. Koronovskii[2], A.E. Hramov[1] and A.G. Balanov[3]
[1]Saratov State Technical University, 410054, Saratov, Russia
[2]Saratov State University, 410012, Saratov, Russia
[3]Department of Physics, Loughborough University, LE11 3TU Loughborough, United Kingdom

***Abstract*—We found the full analytical solution of the semiclassical model, described the stationary profile of the electric field in the miniband semiconductors, subjected to the DC voltage. The analysis of obtained solution shown the three different types of the field distribution, taken place in the semiconductor depending on the emitter current-field characteristics. Among the observed profiles we found the spatially-homogeneous solutions, existed in the condition of the negative differential conductivity (NDC), and represented themselves as the key condition for the THz Bloch oscillations. We applied our theory for the estimation of the current field-condition in the natural SiC superlattice, demonstrated the terahertz electroluminescence and confirmed its Bloch mechanism.**

I. INTRODUCTION

The pioneering work of Esaki and Tsu, published in 1970, [1] drew attention to the fact that the relatively large scale periodic potential in semiconductor superlattices (SLs) made them ideal structures in which The Bloch oscillations can be obtained. So, this kind of semiconductor structures had become the prospective solids served as the background for creating of THz microwave devices.

At the same time, the realization of the coherent Bloch oscillations in SLs is currently problematic due to the instability of the electric field in the condition of NDC. This instability results in a formation of electric domains, which are destructive for the THz Bloch oscillations [2]. Moreover, along with the absence of charge domains, the coherent Bloch oscillations requires the special properties of the field profile, namely, the homogeneous distribution of the electric field.

In this letter we analyze in detail the stationary state of the miniband semiconductor structure and study the possibility of the realization of the uniform field profile in the condition of NDC.

II. RESULTS

A standard mathematical model describing the stationary spatial distributions of the electric field $F(X)$ and the volume electron density $N(X)$ in a one-dimensional solid sample under the conditions of electron injection from a contact includes the Poisson's equation and the current continuity equation, written in form

$$\frac{dF}{dX} = \frac{q}{\varepsilon_0 \varepsilon_r}\left(N - N_D\right), \qquad J = qNV_d(F). \tag{1}$$

Here q - electron charge, ε_r is relative permittivity of the semiconductor. The Eqs. (1) can be rewritten in the dimensionless form as

$$\frac{df}{dx} = \alpha\left[\frac{j(1+f^2)}{f} - 1\right], \tag{2}$$

where f, j - the dimensionless electric field and current density, α - dimensionless NL product [3]. One can see, that the Eq. (2) has two stationary points f_+ and f_-, which satisfy the relation

$$f_{\pm} = \frac{1 \pm \sqrt{1-4j^2}}{2j}. \tag{3}$$

These states are shown in Fig. 1, *a*. One can see, that for the dimensionless value of the current density, which remain less than 1/2, the states f_+ and f_- exist and for the certain conditions the field profile becomes uniform (Fig. 1, *b*, *c*). In case, when j>1/2 these states disappear and the electric field monotonically growths across the structure (Fig. 1, *d*).

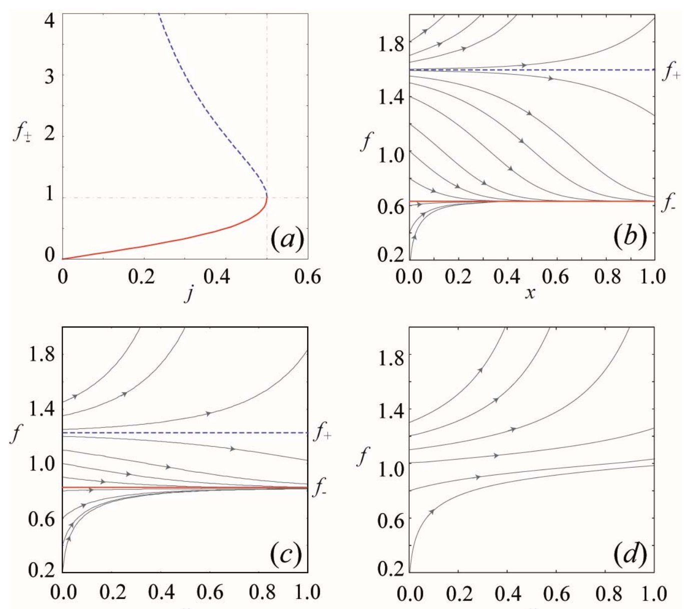

Fig. 1. The location of the points f_- and f_+, which define the uniform field profiles for the different values of the current density (*a*), The solid red and dashed blue lines correspond, respectively, to the f_- and f_+ states. The set of field profiles $f(x)$, obtained for the different values of the emitter electric field $f_e = f(0)$ and different values of the dimensionless current density j: j=0.45 (*b*), j=0.49 (*c*) and j=0.505 (*d*). The uniform profiles, corresponded to the states f_- and f_+, are shown by solid red and dashed blue lines.

The equation (2) has been solved analytically (for details see ref. [3]). We have shown that the distribution of the electric field along the sample can be described via the two different solutions, depending on the value of the current

978-1-4673-8485-8/16/$31.00 ©2016 IEEE

density [3].

Within the developed analytical theory we found out that the shape of the stationary field profile is defined by the values of the current density j, which remains constant on the whole length of the system and the value of the electric field in the emitter $f_e = f(0)$. As the result we have defined three types of the electric field distribution, which take place in the sample for different values of f_e and $j<1/2$.

The spatial electric field distributions of type I occur for $f_e < f_–$. In this case, the value of electric field increases rapidly with the spatial coordinate in the vicinity of the emitter and, approaching the value of $f_–$, remains constant on the rest of the sample. In the case of a low current density j, the field is almost uniform along the greater part of the semiconductor superlattice (Fig. 1, *b*).

The spatial electric field distributions of type II can be obtained in the superlattice for $f_– < f_e < f_+$. They are characterized by a decrease of the electric field strength with an increase of the spatial coordinate x in the vicinity of the emitter. When the value of the current density approaches the peak value of Esaki–Tsu, the states $f_–$ and f_+ converge (see. Fig. 1, *b* and Fig. 1, *c*), and the range of the values of f_e for which the distributions of type II exist becomes narrower. It is important, that in this case the value of electric field within a II-type distribution decreases with the increase of the spatial coordinate rather slowly.

The spatial electric field distributions of type III occur for $f_e > f_+$. In this case, for most of the f_e values, the value of electric field increases rapidly with the increase of the spatial coordinate and achieve high values at the collector of the structure. In order to obtain a quasi uniform field distribution, the corresponding value of emitter electric field f_e has to be very close to f_+.

Finally, when the value of current density reaches the peak value ($j^* = 1/2$), the states $f_\pm$ merge and disappear, which corresponds to a saddle–node bifurcation. The electric field distributions taking place in the superlattice for $j > 1/2$ are shown in Fig. 1, *d*. One can see, that in this case, the value of electric field increases along the entire length of the system. In this case the distribution becomes close to the spatially uniform for the values of the emitter electric field chosen near the critical electric field $f_e = 1$.

Considering the effect of the emitter characteristics on the properties of the electric field profile we use the boundary condition that defines the dependence of f_e on the value of current density according to some electrical characteristic of the injecting contact $j = j_e(f_e)$. As an example of such characteristic, we consider the linear dependence $j = sf_e$, where s is the dimensionless conductance of the emitter.

Fig. 2, *a* shows three typical contact characteristics (straight lines 1–3) along with the Esaki–Tsu curve. The Esaki–Tsu curve may be considered as the combination of the curves $f_–(j)$ and $f_+(j)$ (see Fig. 1, *a*). According to the latter, each point of its intersection with a straight line, where $f_e(j) = f_\pm(j)$, corresponds to those values of the electric field $f(x) = f_e$ and the current density that, for a given parameter s, determine the spatially uniform solution. Furthermore, regions I, II, and III on the plane (f_e, j) correspond to the boundary conditions for which the three previously described types of the electric field distribution are implemented.

One can see that straight line 1, which describes an ohmic contact, lies in region I and, thus, cannot intersect the f_+ curve. This illustrates that a uniform field distribution cannot be attained under the conditions of negative differential mobility in a structure with a purely ohmic contact. Straight line 2 (for $j < 0.5$) lies mostly in region II close to the $f_–$ curve and intersects it at $j \approx 0.47$. In this case, both type-I and type-II distributions may occur. Straight line 3, corresponding to a contact with a low conductance, intersects the f_+ curve at $j \approx 0.3$. In this case, $f_e > 1$, which corresponds to the condition of negative differential mobility $\mu_d < 0$.

Having analyzed the recent experiment [4], in which the 1.5-2.0 THz emission was obtained from the natural SiC superlattice for a current of I = 210 mA and the sample parameters: d = 0.75 nm, Δ = 260 meV, $N_D = 10^{16}$ cm^{-3}, the cross-sectional area $S = 3 \times 10^{-5}$ cm^{-2} and $\tau = 3 \times 10^{-13}$ s, we have found $j = 0.3 < 1/2$ and, according to Eq. (5), $f_+ = 3$ or F_+ = 87 kV/cm. This value is close to the estimate $F_{\rm rad}$ = 84 kV/cm of the field corresponding to the onset of generation obtained in [4] directly from the analysis of the experimental data. Taking into account, that the considered SiC superlattice [4] has a nonohmic injecting contact in which the nonlinearity of the electrical characteristic is caused by the breakdown of impurity centers, one can confidently associate the emission of the terahertz radiation observed in [4] with a transition of the SiC superlattice into a spatially uniform state.

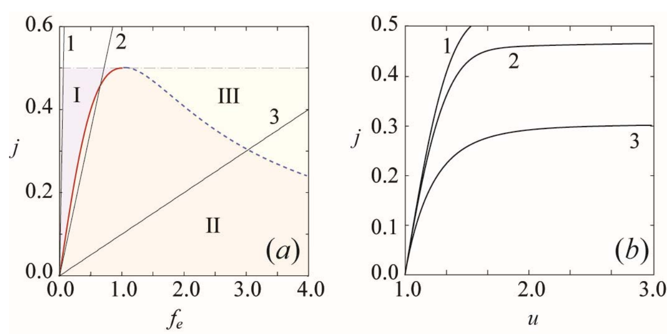

Fig. 2. (*a*) Three regions in the parameter plane (f_e, j), $j \le 1/2$, corresponding to the field distributions of three different types I, II, and III, the Esaki–Tsu curve (red solid and blue dashed lines) and linear characteristics of the emitters with the dimensionless conductances s = 17 (1), s = 0.7 (2), and s = 0.1 (3). (*b*) The Current–voltage characteristics $j(u)$ of the superlattice corresponding to contact electrical characteristics 1–3.

This work is supported by the Russian Foundation for Basic Research (grant 16-32-80125).

References

[1] L. Esaki and R. Tsu, “Superlattice and negative differential conductivity in semiconductors” *IBM J. Res. Dev,* vol. 14, pp. 61-65, 1970

[2] M. Büttiker and H. Thomas, “Current Instability and Domain Propagation Due to Bragg Scattering” *Phys. Rev. Lett*, vol. 38, p. 78, January 1977

[3] V.A. Maksimenko, V.V. Makarov, A.A. Koronovskii, A.E. Hramov, R. Venkevichius, G. Valushis, A.G. Balanov, F.V. Kusmartsev, K.N. Alekseev “Electric-Field Distribution in a Quantum Superlattice with an Injecting Contact: Exact Solution” *JETP Letters*, vol. 103 (7), pp. 465–470, 2016

[4]. V.I. Sankin, A.V. Andrianov, A.O. Zakhar`in and A.G. Petrov, “Terahertz electroluminescence from 6H-SiC structures with natural superlattice” *Appl. Phys. Lett.*, vol. 100, p. 111109, March 2012